Preparation and Characterization of Activated Carbon Fibers from Liquefied Wood by $ZnCl_2$ Activation

Zhigao Liu, Yuxiang Huang, and Guangjie Zhao*

In this study, activated carbon fibers (ACFs) were prepared from liquefied wood by chemical activation with $ZnCl_2$, with a particular focus on the effects of temperature and $ZnCl_2$: liquefied wood-based fiber (LWF) ratio on yield, porous texture, and surface chemistry. The characterization and properties of these ACFs were investigated by nitrogen adsorption/desorption, Fourier transform infrared (FTIR) spectroscopy, and X-ray photoelectron spectroscopy (XPS). When using a 6:1 impregnation ratio, the specific surface area (S_{BET}) of the resultant ACFs was as high as 1423 m^2/g. The effect of an increase in impregnation ratio on the porosity of ACFs was stronger than that of an increase in the activation temperature. However, the former had a weaker impact on the surface chemistry and structure. It was also found that the yields of ACFs obtained by $ZnCl_2$ activation were higher than those obtained by physical activation. Besides, the prepared ACFs presented higher adsorption than other raw materials in the adsorption test, indicating that ACFs prepared from LWF by $ZnCl_2$ activation could be used as an adsorbent for the adsorption of medium size organic compounds.

Key words: Activated carbon fibers (ACFs); Liquefied wood; $ZnCl_2$ activation; Porosity; Surface properties

*Contact information: College of Materials Science and Technology, Beijing Forestry University, Tsinghua East Road 35, Haidian District, 100083, Beijing, China; *Corresponding author: zhaows@bjfu.edu.cn*

INTRODUCTION

Activated carbon fibers (ACFs) are applied efficiently in various industries, particularly for removing pollutants from water and air (Saeidi and Lotfollahi 2015). Their applications have been widely extended, not only as adsorbents but also as electronic materials because of their high surface area and abundant functional surface groups (Avelar *et al.* 2010).

Various kinds of materials can be utilized to produce ACFs such as phenolic fibers, pitch fibers, viscose fibers, and polyacrylonitrile fibers. Meanwhile, oil, natural gas, and other non-renewable resources are being depleted, and natural disasters and environmental problems are become increasingly serious. Thus, more and more biomass resources such as palm, cotton, and bamboo have been used to prepare ACFs by researchers.

Wood, as one of the most abundant renewable resources on the earth (Aber *et al.* 2009), has been used in the preparation of ACFs. The study of wood-based ACFs can be dated to the middle of last century. Abbott successfully produced viscose-ACFs from cellulose in 1962. Then Uraki *et al.* (2001) prepared ACFs from softwood acetic acid lignin.

However, the methods just mentioned, which require the separation of the lignin and cellulose from wood before developing ACFs, show considerable disadvantages such as having a complex process and low resource utilization. Liquefied wood, which does not require the separation of chemical components of wood and leads to higher wood utilization ratios (Alma *et al.* 1995, 2001; Ma and Zhao 2008), has also been tested for ACF production. Besides, appearance of liquefaction technology of wood has provided a large number of wood wasters and wood processing residues with a new space for development.

Currently, ACFs can be produced by physical or chemical activation. Physical activation is done by carbonization of carbon precursors in an inert atmosphere to remove non-carbon elements, followed by activation in the presence of oxidizing gasifying agents at a higher temperature (Wang and Kaskel 2012). Chemical activation is generally conducted by impregnating with chemical agents such as alkali (KOH, K_2CO_3), alkali earth metal salts ($AlCl_3$, $ZnCl_2$, and $FeCl_3$), or certain acids (H_3PO_4, H_2SO_4), where the porosity is developed by dehydration reactions of the activating reagent (Li *et al.* 2015). Compared to physical activation, chemical activation provides higher yields under a lower activating temperature and results in less surface damage during the activation of fiber (Mohanty *et al.* 2005).

To obtain a high surface area, $ZnCl_2$ has been used as activating reagent among the chemical activating agents (Liu *et al.* 2014; Isilay Ozdemir *et al.* 2014; Kumar and Mohan Jena 2015). More and more researchers have prepared activated carbon or activated carbon fiber from biomass resource by chemical activation with $ZnCl_2$. Yorgun Sait *et al.* (2009) reported the preparation of activated carbon from *Paulownia* wood by $ZnCl_2$ activation. The influences of carbonization temperature and impregnation ratio were investigated. Du *et al.* (2013) prepared activated carbon hollow fibers from renewable ramie fibers (RFs) by $ZnCl_2$ activation under lower temperature. Isilay *et al.* (2014) prepared activated carbon from the grape stalk by chemical activation with $ZnCl_2$ and found that the carbonization temperature and impregnation ratio had significant effects on the surface area and pore structure.

In recently years, preparation of ACFs from liquefied wood using steam and KOH activation has been studied (Jin and Zhao 2014a,b; Huang and Zhao 2015). However, there has been a lack of reports dealing with the preparation of ACFs from liquefied wood by $ZnCl_2$ activation.

As we know from previous studies, $ZnCl_2$ has the potential to lower the activating temperature and improve the yield of ACF. The porous structure and adsorption capacity of the ACFs prepared by KOH activation, steam activation, and $ZnCl_2$ activation are various. Therefore, the preparation of ACFs from the same starting material by chemical activation, using $ZnCl_2$ as the activating agent, was investigated in present study.

The effects of process parameters such as the $ZnCl_2$/fiber ratio (impregnation ratio) and activation temperature on the porosity, yields, and surface properties of the resultant products were also examined. Moreover, the adsorption performance of prepared samples were tested for the adsorption of methylene blue and compared with others published in the literature.

EXPERIMENTAL

Materials

Chinese fir (*Cunninghamia lanceolata*) was used as a raw material, sourced from Fujian, China. All chemicals used in the study were purchased from Beijing Chemical Works, Beijing, China. They were all of reagent grade and used without further purification.

Methods

Liquefied wood based fibers (LWFs) were prepared from Chinese fir through a process that included liquefaction, melt-spinning, and curing, according to a previous study by the authors (Huang *et al.* 2015b). In the impregnation of LWFs, 50 mL of $ZnCl_2$ aqueous solution was brought into contact with about 2 g of the material. The amount of activating agent present in such a solution was that corresponding to a given $ZnCl_2$:LWF ratio (3:6 by weight). Then, $ZnCl_2$-impregnated LWFs were placed in a horizontal transparent tube furnace (Y02PB, Thermcraft Inc., USA) and heated from room temperature to 700 °C in a N_2 atmosphere. The heating rate was 4 °C /min, and the holding time at 700 °C was 1 h. The produced samples were washed in 1 mol/L HCl, rinsed several times in distilled water until the pH of wash water became neutral, and then dried in an oven at 110 °C for 24 h to obtain the ACFs. The resultant ACFs were designated ZL*, where * represents the impregnation ratio. Another series of ACFs was prepared by maintaining the $ZnCl_2$:LWF ratio (4:1 by weight) and varying the activation temperature in the range of 500 to 800 °C. These ACFs were denoted Z*, where * represents the activation temperature. The final yield was determined as the weight ratio of ACFs to LWFs.

The specific surface area and pore structure characteristic of the prepared ACFs were determined by N_2 adsorption-desorption isotherms at -196 °C (Autosorb-iQ, Quantachrome, USA). Before analysis, the samples were degassed at 300 °C for 3 h. The surface area (S_{BET}) of prepared ACFs was estimated by BET method. The total pore volume (V_{total}) was estimated to be the liquid volumes of N_2 at high relative pressure (P/P_0=0.995). The t-plot analysis method was used to calculate the micropore specific surface (S_{micro}) and micropore volume (V_{micro}). The mesopore surface area (S_{meso}) and the mesopore volume (V_{meso}) were calculated by the BJH method. The pore size distribution (PSD) of the prepared ACFs has been determined by the density functional theory (DFT) method.

XPS analysis was performed using a spectrophotometer (Escalab 250Xi, Thermo Scientific, USA) with a monochromated AlKα X-ray source (hv = 1486.6 eV; 10 mA, 13 kV). The survey scans were collected from a binding energy ranging from 0 to 1350 eV. The chemical groups of the samples were recorded between 4000 and 400 cm^{-1}, using a Fourier transform infrared spectrum analysis spectrometer (FTIR, Bruker Tensor 27, Germany). The KBr pellet method, with 5% of samples, was applied. The samples were pulverized (100-mesh) and mixed with KBr before pellet preparation.

The adsorption capacity of prepared samples was tested for the adsorption of organic compound (methylene blue, $C_{20}H_{19}ClN_4$). The tests were performed in a set of Erlenmeyer flasks (100 mL) where 25 mL of MB solutions with concentration of 1200 mg/L were placed in these flasks. About 3 mg of ACFs was added to each flask and maintained under agitation at 150 rpm for 30 min at 25 °C. After filtration, the

determination of the remaining concentrations was made by UV-visible spectroscopy (Biowave II, WPA, England) for methylene blue (λ=665nm).

RESULTS AND DISCUSSION

Yield of ACFs

The product yields of ACFs prepared from liquefied wood are shown in Table 1. It can be observed that the ACFs obtained by $ZnCl_2$ activation had higher yields than those obtained by physical activation (Jin and Zhao 2014a,b; Ma *et al.* 2014). The activation temperature and impregnation ratio play a major role on the yield of ACFs. From Table 1, with increasing the impregnation ratio from 3 to 6 at 700 °C, more carbon burn-off occurred and there was micropore widening into mesopores in the presence of extra $ZnCl_2$, resulting in lower yield values (Kumar and Mohan Jena 2015). On the contrary, activation with a low $ZnCl_2$ impregnation ratio resulted in a higher yield of 53.79% to 62.97% because $ZnCl_2$ selectively stripped H and O away from the impregnated sample as H_2O and H_2 rather than hydrocarbons, CO or CO_2. As the activated temperature was increased from 500 °C to 800 °C, the yield of ACFs also decreased, since the promotion of tar volatilization by higher temperature. These results are in good agreement with that reported by previous studies (Qian *et al.* 2007; Sait *et al.* 2009).

Table 1. Specific Surface Area (SSA) and Pore Volume of Activated Carbon Fibers Prepared from Liquefied Wood at Various Activation Temperatures and Impregnation Ratios

	SSA (m^2/g)			Pore volume (cm^3/g)			Yield(%)
Sample	S_{BET}	S_{micro}	S_{meso}	V_{total}	V_{micro}	V_{meso}	
Z500	837	619	135	0.498	0.286	0.14	66.4
Z600	957	729	162	0.502	0.302	0.163	63.31
Z700	1086	796	258	0.598	0.326	0.251	53.79
Z800	1268	916	349	0.739	0.391	0.341	45.1
ZL3	810	587	196	0.446	0.237	0.191	62.97
ZL4	1086	796	258	0.598	0.326	0.251	53.79
ZL5	1356	829	418	0.872	0.371	0.439	48.36
ZL6	1423	836	586	0.953	0.376	0.566	44.41

N_2 Adsorption/Desorption Isotherm

The N_2 adsorption/desorption isotherms measured for $ZnCl_2$-activated ACFs at various activating temperature and impregnation ratios are shown in Figs. 1 and 2. For Z500 and Z600, the volume absorbed increased quickly with increasing pressure at low relative pressures but it leveled off when the relative pressure was above 0.1. This means that the isotherms were typical type I isotherms, according to the well-known IUPAC classification (Sing *et al.* 1985). However, the isotherms ranged in general from Type I isotherms at low temperature to Type IV isotherms as the activating temperature was increased. This indicated that the prepared ACFs demonstrated mainly a micropore

structure at low temperature but developed a mesopore structure at high temperature (Williams and Reed 2006).

As shown in Fig. 2, the absorbed volume of ACFs maintained a linear upward trend when the relative pressure is above 0.1, indicating that the isotherms belong to the non-microporous type. Moreover, their isotherms are characterized by both a broader knee and an adsorption/desorption hysteresis loop, corresponding to a combination of Type I and IV isotherm, suggesting the co-existence of micropores and mesopores (Huang *et al.* 2015b).

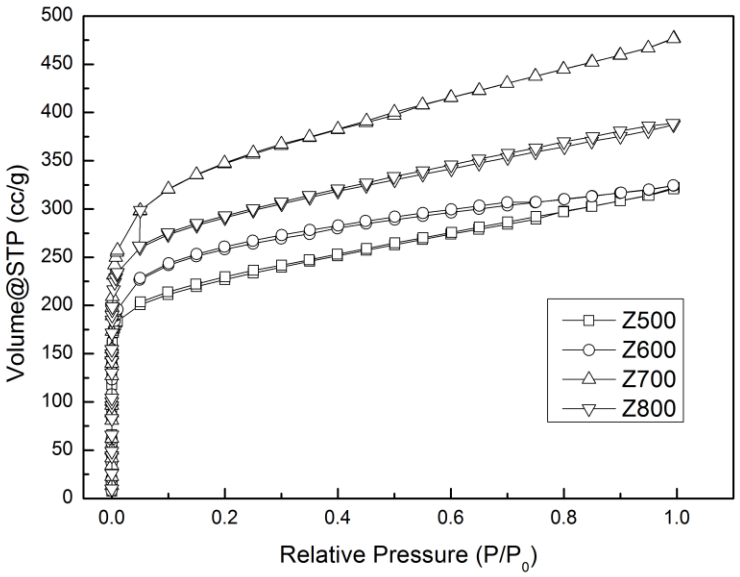

Fig. 1. Nitrogen adsorption-desorption isotherms of liquefied wood-based activated carbon fibers at various activation temperature

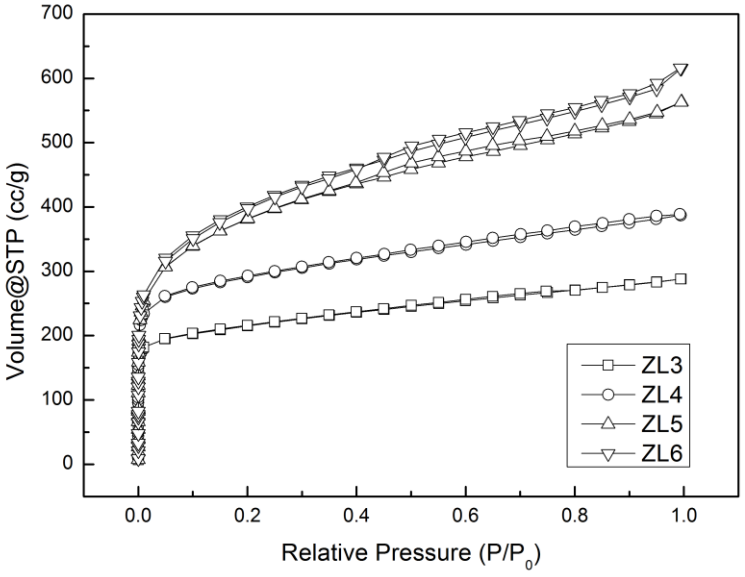

Fig. 2. Nitrogen adsorption-desorption isotherms of liquefied wood-based activated carbon fibers at various impregnation ratios

Pore Structure

The pore properties of all the $ZnCl_2$-activated ACFs, including S_{BET}, S_{micro}, S_{meso}, V_{tot}, V_{micro}, and V_{meso}, are listed in Table 1. From Table 1, the S_{BET}, S_{micro}, S_{meso}, and V_{tot} of ACFs gradually increased with increasing activating temperature from 500 °C to 800 °C at a 4:1 impregnation ratio. The $ZnCl_2$ works as dehydration reagent that lowers the activating temperature during chemical activation and restricts the formation of tar as well as promotes charring of carbon (Kumar and Mohan Jena 2015). LWFs had formed a relatively stable carbon structure below 400 °C by using $ZnCl_2$ as an activating agent. Then the $ZnCl_2$ began to erode the carbon matrix to develop porosity between 400 and 500 °C (Zhang *et al.* 2006). Nevertheless, when the temperature was higher, the mechanism of activation was different: $ZnCl_2$ was vaporized and decomposed into zinc and chlorine, which can further create and enlarge the pores (Zhang *et al.* 2009). It is apparent from the data shown in Table 1 that using $ZnCl_2$ as an activating agent was very efficient to produce ACFs with high porosity and high surface area and that the $ZnCl_2$:LWF ratio had a positive effect on the development of the porosity. The S_{BET} and V_{tot} underwent an increase with increasing impregnation ratio from 1 to 4 at 700 °C. This is because the concentration of $ZnCl_2$ attached to the fiber surface increased as the impregnation ratio increased, which would result in a more violent activation reaction. However, when the ratio was above 5, this increase was not obvious any more. The percentage of increase (SZL6-SZL5)/ZL5) in S_{BET} was only 4.9%. Because of the limited amount of carbon in the sample, it was not possible to increase the specific surface area indefinitely with increasing impregnation ratios. Similar results have been reported by Zhang *et al.* (2006), who studied the preparation of activated carbon from sawdust activated with $ZnCl_2$. The S_{BET} of ZL6 was as high as 1423 m^2/g, which was higher than that of Z800, indicating that the effect of an increase in impregnation ratio on the porosity of ACFs was stronger than that of the increase in the activation temperature.

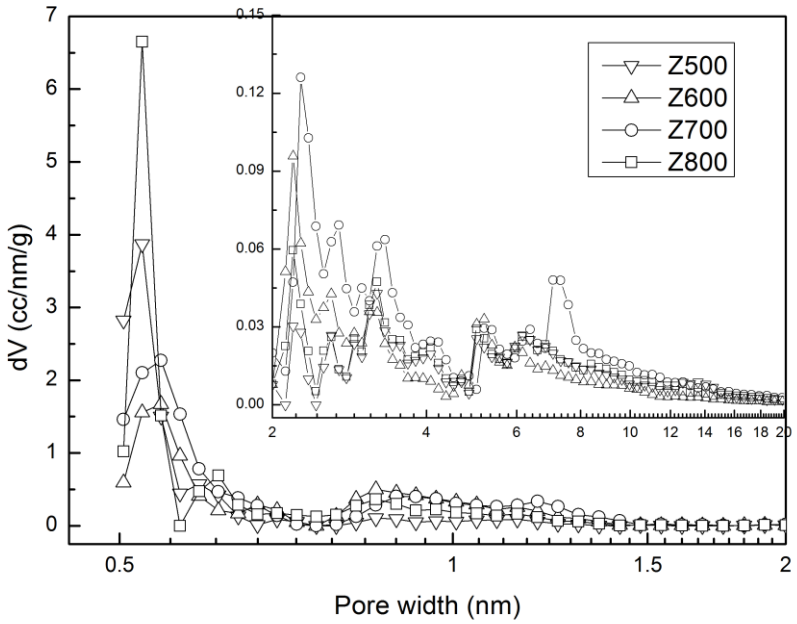

Fig. 3. Pore size distribution plots for activated carbon fibers from liquefied wood at various activation temperatures

The pore size distribution (PSD) in the micropore range was very similar for all the $ZnCl_2$-activated ACFs, where micropores mostly accumulated from 0.5 to 1.5 nm. However, a clear difference can be observed in the mesopore region (2 to 20 nm), where multiple peaks appear. As seen in Fig. 3, the micropore volume increased with increasing temperature. However, the number of ultramicropores, with pore sizes from 0.5 to 0.7 nm, decreased when the activating temperature reached 800 °C. At this high temperature, a great amount of $ZnCl_2$ had been vaporized and decomposed, which may result in these ultramicropores being enlarged. It is also clear that, as the temperature was increased, the mesopore size distribution widened and the mesopore volume increased correspondingly. This indicates that more mesopores will be generated when high activating temperature is applied. Similar to the ACFs activated at various temperatures, micropores also primarily accumulated from 0.5 to 1.5 nm for the ACFs activated with various $ZnCl_2$:LWF ratios (Fig. 4). The pore volume decreased with increasing impregnation ratio in the micropore region, with pore sizes of 0.5 to 0.7 nm, whereas in the range of 0.8 to 1.5 nm, the pore volume increased. This indicates that some micropores with small pore sizes were enlarged to those of larger size because of the more violent activation reaction as the impregnation ratio increased. At the same time, in the wide range of 3 to 20 nm, the pore volumes of ZL5 and ZL6 were considerably higher than those of the other two samples, indicating the $ZnCl_2$: LWF ratio had a noticeable impact on the PSD in this region.

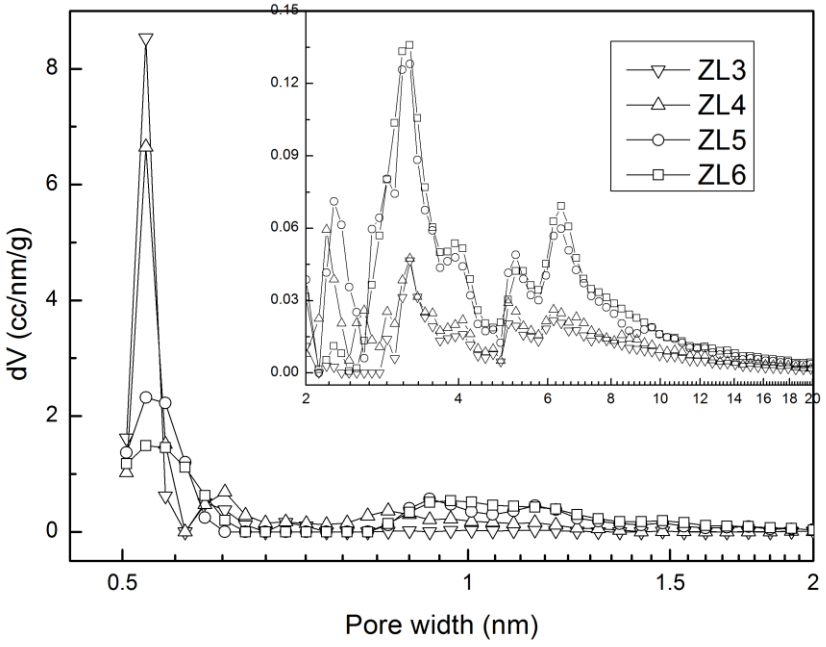

Fig. 4. Pore size distribution plots for activated carbon fibers from liquefied wood at various impregnation ratios

XPS Analysis of ACFs

The XPS spectra of $ZnCl_2$-activated ACFs with various activating temperatures are shown in Fig. 5. It is apparent that the element C was the most dominant constituent in all samples, and O was the second. Atomic concentrations on the surface of the ACFs are summed up in Table 2. With increasing activating temperature, carbon content increased

from 87.8% to 93.0%, while the oxygen content decreased from 10.4% to 5.8%, which gives an explanation for the decrease in the O/C atomic ratio. This can be ascribed to the catalytic dehydration and dehydrogenation of $ZnCl_2$. The element O was lost from the surface as water or other products. This implies that although more carbon could be consumed by reacting with $ZnCl_2$ when the concentration increased, the oxygen of the ACFs themselves was subjected to a greater loss. From Table 2, the carbon content increased from 88.5% to 93.4%, while the oxygen content decreased from 9.6% to 5.6% and O/C ratio also decreased from 10.8% to 6.0%, suggesting that the impregnation effect was similar to the temperature effect. An increase in the impregnation ratio would strengthen the erosion effect on the fiber surface by $ZnCl_2$, thereby causing a more pronounced catalytic dehydration and dehydrogenation. $ZnCl_2$, as an activating agent, would selectively strip H and O away from the raw material as H_2O and H_2 rather than CO, CO_2, or hydrocarbons (Qian *et al.* 2007; Kumar *et al.* 2015). Thus, more O than C would be lost.

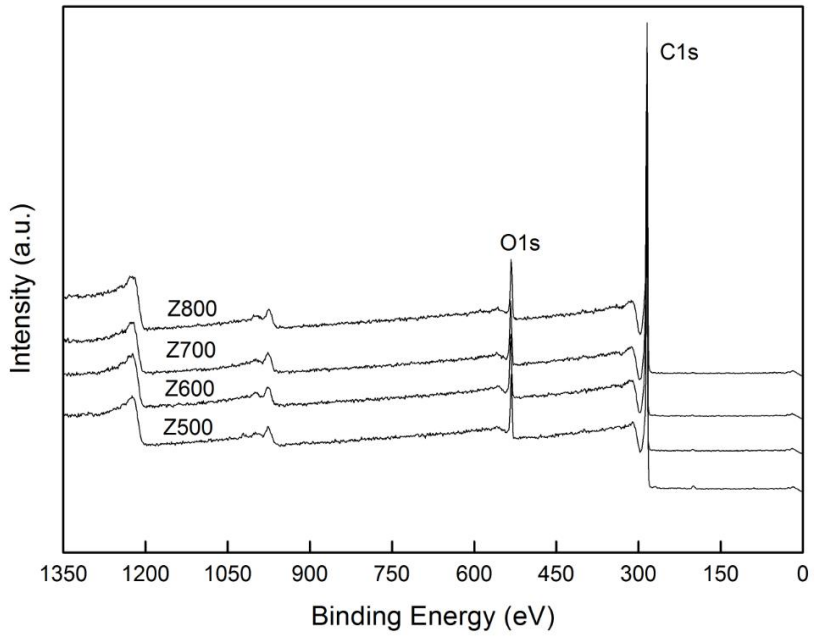

Fig. 5. XPS curve of ACFs from liquefied wood

Table 2. Surface Element Content and Oxygen/Carbon Ratio of Activated Carbon Fibers from Liquefied Wood at Various Activation Temperatures and Impregnation Ratios

	Element content (%)					
Sample	C	O	N	Zn	Cl	O/C
Z500	87.84	10.4	1.18	0.12	0.47	11.84%
Z600	89.63	8.39	1.31	0.18	0.5	9.36%
Z700	90.68	7.99	0.95	0.1	0.27	8.81%
Z800	92.96	5.76	1.04	0.06	0.17	6.20%
ZL3	88.5	9.55	0.77	0.1	0.48	10.79%
ZL4	90.68	7.99	0.95	0.1	0.27	8.81%
ZL5	93.17	5.86	0.66	0.06	0.25	6.29%
ZL6	93.4	5.63	0.71	0.06	0.2	6.03%

FTIR Analysis of Precursor Fiber and Prepared Activated Carbon Fibers

The 4000 to 400 cm^{-1} infrared spectral regions of the $ZnCl_2$-activated ACFs prepared at various temperatures and impregnation ratios are shown in Figs. 6 and 7.

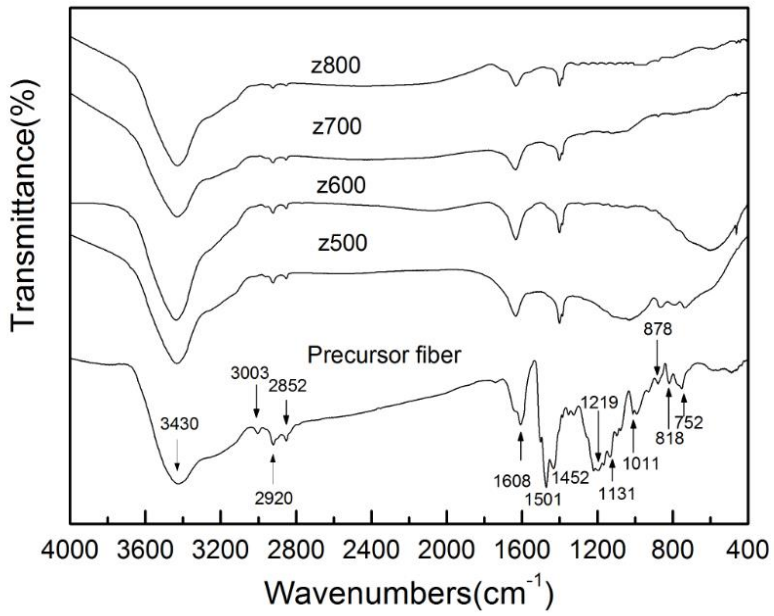

Fig. 6. FTIR spectra of activated carbon fibers at various temperatures

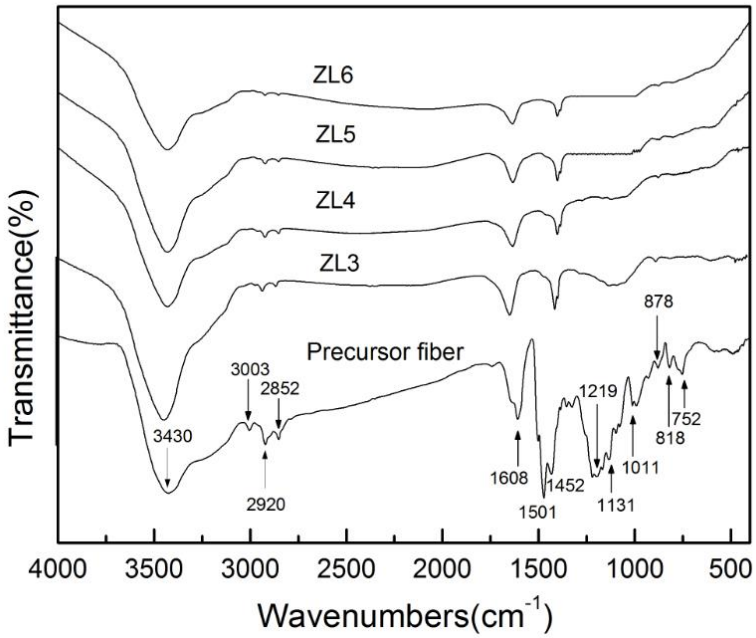

Fig. 7. FTIR spectra of activated carbon fibers at various impregnation ratios

For the precursor fiber, a lot of peaks can be observed, suggesting that there were more complicated constitutions and structures of the precursor fiber due to the multifarious components of wood and various reactions, such as degradation, phenolation, and polycondensation during liquefaction (Huang *et al.* 2015a). A broad peak located at

3430 cm^{-1} was assigned to the stretching vibration of hydroxyl, and a group of bands could be observed between 900 cm^{-1} and 650 cm^{-1}, characteristic of the out-of-plane bending vibration of C-H in aromatic rings (Domínguez *et al.* 2013), with three peaks at 878, 818, and 752 cm^{-1}. The peak at 878 cm^{-1} can be assigned to isolated H in the aromatic rings, and the band at 818 cm^{-1} is related to 1,4- and 1,2,4- substitutions in aromatic rings. The strong peak at 752 cm^{-1} corresponds to disubstituted-1,2 in aromatic rings. As the temperature rises, the peaks related to C-H out-of-plane bending of aromatic rings at 900 to 650 cm^{-1} disappeared, indicating that a multi-benzene fused ring structure formed. The spectrum of precursor fiber exhibited multiple bands in the region of 1300 to 1000 cm^{-1}, where the band is quite difficult to be identified because it may be ascribed to C-O in acids, alcohols, phenols, ethers, or ester groups. The CO groups are very sensitive to the increase in temperature, as they are absent from Z600, Z700, and Z800. The FTIR spectra are similarly shaped for the ZN samples, which demonstrates that preparation of ACFs from LWFs by varying the $ZnCl_2$:LWF ratio is not an effective method to modify the surface functional groups compared with varying the activation temperature.

Adsorption Capacity of ACFs

The MB adsorptions of all the prepared ACFs are shown in Table 3. With increasing of the impregnation ratio from 3 to 6 at 700 °C, MB adsorption of sample increased slightly. For Z500-Z800, the MB adsorption of prepared sample increased as the activating temperature was increased from 500 °C to 700 °C, but decreased at 800 °C. These results are consistent with pore size distribution plots for ACFs. Besides, ACFs prepared from liquefied wood presented higher adsorption for methylene blue than other raw materials (*Pinus sylvestris*, 1344 cm^2/g, 299 mg/g; Piassava fibers, 1190 cm^2/g, 277 mg/g; Coffee husks, 1522 cm^2/g, 263 mg/g) in the published literature (Oliveira *et al.* 2009; Avelar *et al.* 2010; Açıkyıldız *et al.* 2014). Thus, ACFs prepared from LWF by $ZnCl_2$ activation would be used as an adsorbent for the adsorption of medium size organic compounds.

Table 3. Adsorption Capacity for MB of Prepared ACFs

Samples	Activating temperature	Impregnation Ratio ($ZnCl_2$/Precursor)	S_{BET}	Q(mg/g)
ZL3	700	3	810	251
ZL4	700	4	1086	359
ZL5	700	5	1356	560
ZL6	700	6	1423	641
Z500	500	4	837	174
Z600	600	4	957	250
Z700	700	4	1086	359
Z800	800	4	1268	282

CONCLUSIONS

1. ACFs with high specific surface and higher yields were prepared from liquefied wood by $ZnCl_2$ activation. When using a 6:1 impregnation ratio and activation temperature of 700 °C, the specific surface are of resultant ACFs (ZL6) was 1423 m^2/g. The

specific surface are of ACFs (Z800) was also as high as 1268 m^2/g when using a 4:1 impregnation ratio and activation temperature of 800 °C.

2. Compared with varying the activation temperature, the method associated with varying the impregnation ratio had a greater effect on the porosity of ACFs, whereas the opposite applies to the impact on the surface functional groups and structures.
3. ACFs prepared from liquefied wood would be used as a good adsorbent for the adsorption of medium size organic compounds.

ACKNOWLEDGEMENTS

This research was financially supported by the Key Projects in the National Science & Technology Pillar Program during the Twelfth Five-year Plan Period, "Key technology and application demonstration for the production of wood-based functional adsorption materials" (2015BAD14B06).

REFERENCES CITED

Aber, S., Khataee, A., and Sheydaei, M. (2009). "Optimization of activated carbon fiber preparation from kenaf using K_2HPO_4 as chemical activator for adsorption of phenolic compounds," *Bioresour. Technol*. 100(24), 6586-6591.DOI: 10.1016/j.biortech.2009.07.074.

Açıkyıldız, M., Gürses, A., and Karaca, S. (2014). "Preparation and characterization of activated carbon from plant wastes with chemical activation," *Microporous and Mesoporous Materials* 198, 45-49. DOI: 10.1016/j.micromeso.2014.07.018

Alma, M. H., Batirk, M. A., and Shiraishi, N. (2001). "Co-condensation of NaOH-catalyzed liquefied wood wastes, phenol, and formaldehyde for the production of resol-type adhesives," *Industrial & Engineering Chemistry Research* 40(22), 5036-5039. DOI: 10.1021/ie000858x

Alma, M., Yoshioka, M., Yao, Y., and Shiraishi, N. (1995). "Preparation and characterization of the phenolated wood using hydrochloric acid (HCl) as a catalyst," *Wood Science and Technology* 30(1), 39-47.DOI: 10.1007/BF00195267

Avelar, F. F., Bianchi, M. L., Gon Alves, M., and Da Mota, E. G. (2010). "The use of piassava fibers (*Attalea funifera*) in the preparation of activated carbon," *Bioresour. Technol.* 101(12), 4639-4645. DOI: 10.1016/j.biortech.2010.01.103

Domínguez, J. C., Oliet, M., Alonso, M. V., Rojo, E., and Rodríguez, F. (2013). "Structural, thermal and rheological behavior of a bio-based phenolic resin in relation to a commercial resol resin," *Ind. Crop. Prod.* 42, 308-314. DOI: 10.1016/j.indcrop.2012.06.004

Du, X., Zhao, W., Wang, Y., Wang, C., Chen, M., Qi, T., Hua, C., and Ma, M. (2013). "Preparation of activated carbon hollow fibers from ramie at low temperature for electric double-layer capacitor applications," *Bioresource Technology* 149, 31-37. DOI: 10.1016/j.biortech.2013.09.026

Huang, Y., and Zhao, G. (2015). "Preparation and characterization of activated carbon fibers from liquefied wood by KOH activation," *Holzforschung* (published online). DOI: 10.1515/hf-2015-0051

Huang, Y., Ma, E., and Zhao, G. (2015a). "Thermal and structure analysis on reaction mechanisms during the preparation of activated carbon fibers by KOH activation from liquefied wood-based fibers," *Ind. Crop. Prod.* 69, 447-455. DOI: 10.1016/j.indcrop.2015.03.002

Huang, Y., Ma, E., and Zhao, G. (2015b). "Preparation of liquefied wood-based activated carbon fibers by different activation methods for methylene blue adsorption," *RSC Adv.* 5(86), 70287-70296. DOI: 10.1039/c5ra11945f

Jin, Z., and Zhao, G. (2014a). "Porosity evolution of liquefied wood-based activated carbon fiber. Part I: Water steam activation at 600-800 °C," *BioResources* 9(2), 2237-2247. DOI: 10.15376/biores.9.2.2237-2247

Jin, Z., and Zhao, G. (2014b). "Porosity evolution of liquefied wood-based activated carbon fiber. Part II: Water steam activation at 850-950 °C," *BioResources* 9(4), 6831-6840. DOI: 10.15376/biores.9.4.6831-6840

Kumar, A., and Mohan Jena, H. (2015). "High surface area microporous activated carbons prepared from Fox nut (*Euryale ferox*) shell by zinc chloride activation," *Applied Surface Science* 356, 753-761. DOI: 10.1016/j.apsusc.2015.08.074

Liu, J., Wang, S. P., Yang, J. M., Liao, J. J., Lu, M., Pan, H. J., and An, L. (2014). "$ZnCl_2$ activated electrospun carbon nanofiber for capacitive desalination," *Desalination* 344, 446-453. DOI: 10.1016/j.desal.2014.04.015

Li, J., Ng, D. H. L., Song, P., Kong, C., Song, Y., and Yang, P. (2015). "Preparation and characterization of high-surface-area activated carbon fibers from silkworm cocoon waste for Congo red adsorption," *Biomass Bioenerg.* 75, 189-200. DOI: 10.1016/j.biombioe.2015.02.002

Ma, X., and Zhao, G. (2008). "Structure and performance of fibers prepare from liquefied wood in phenol," *Fibers and Polymers.* 9(4), 405-409. DOI*:* 10.1007/s12221-008-0065-6

Ma, X., Zhang, F., Zhu, J., Yu, L.., and Liu, X. (2014). "Preparation of highly developed mesoporous activated carbon fiber from liquefied wood using wood charcoal as additive and its adsorption of methylene blue from solution," *Bioresource Technology* 164, 1-6. DOI: 10.1016/j.biortech.2014.04.050

Mohanty, K., Jha, M., Meikap, B. C., and Biswas, M. N. (2005). "Removal of chromium (VI) from dilute aqueous solutions by activated carbon developed from *Terminalia arjuna* nuts activated with zinc chloride," *Chemical Engineering Science* 60(11), 3049-3059. DOI: 10.1016/j.ces.2004.12.049

Oliveira, L. C. A., Pereira, E., Guimaraes, I. R., Vallone, A., Pereira, M., Mesquita, J. P., and Sapaq, K. (2009). "Preparation of activated carbons from coffee husks utilizing $FeCl_3$ and $ZnCl_2$ as activating agents," *Journal of Hazardous Materials* 165(1-3), 87-94. DOI: 10.1016/j.jhazmat.2008.09.064

Ozdemir, I., Şahin, M., Orhan, R., and Erdem, M. (2014). "Preparation and characterization of activated carbon from grape stalk by zinc chloride activation," *Fuel Processing Technology* 125, 200-206. DOI: 10.1016/j.fuproc.2014.04.002

Qian, Q., Machida, M., and Tatsumoto, H. (2007). "Preparation of activated carbons from cattle-manure compost by zinc chloride activation," *Bioresource Technology* 98(2), 353-360. DOI: 10.1016/j.biortech.2005.12.023

Saeidi, N., and Lotfollahi, M. N. (2015). "Effects of powder activated carbon particle size on adsorption capacity and mechanical properties of the semi activated carbon fiber," *Fiber Polym.* 16(3), 543-549. DOI: 10.1007/s12221-015-0543-6

Sing, K. S. W., Everett, D. H., Haul, R. A. W., Moscou, L., Piepotti, R. A., Rouqu Erol, J., and Siemieniewska, T. (1985). "Reporting physisorption data for gas/solid systems with special reference to the determination of surface area and porosity," *Pure Appl. Chem.* 57(11), 603-619. DOI: 10.1351/pac198557040603

Uraki, Y., Nakatani, A., Kubo, S., and Sano, Y. (2001). "Preparation of activated carbon fibers with large specific surface area from softwood acetic acid lignin," *Journal of Wood Science* 47(6), 465-469. DOI: 10.1007/BF00767899

Williams, P., and Reed, A. (2006). "Development of activated carbon pore structure *via* physical and chemical activation of biomass fibre waste," *Biomass and Bioenergy* 30(2), 144-152. DOI: 10.1016/j.biombioe.2005.11.006

Wang, J., and Kaskel, S. (2012). "KOH activation of carbon-based materials for energy storage," *J. Mater. Chem.* 22, 23710-23725. DOI: 10.1039/c2jm34066f

Yorgun, S., Vural, N., and Demiral, H. (2009). "Preparation of high-surface area activated carbons from Paulownia wood by $ZnCl_2$ activation," *Microporous and Mesoporous Materials* 122(1-3), 189-194. DOI: 10.1016/j.micromeso.2009.02.032

Zhang, H., Ye, L., and Yang, L. (2006). "Preparation of activated carbon from sawdust by chemical activation with zinc chloride," *Materials Science Technology* 14(1), 42-45.

Zhang, Z., Zhu, Y., Liu, H., Wang, D., Liang, M., and Liang, Y. (2009). "Preparation of activated carbon from bagasse by activation with zinc chloride," *Environ. Protect. Chem. Ind.* 29(1), 62-66.

Article submitted: September 17, 2015; Peer review completed: December 29, 2015; Revised version received: February 1, 2016; Accepted: February 2, 2016; Published: February 10, 2016.
DOI: 10.15376/biores.11.2.3178-3190